STABILITY IN FLUTTER OF HOVERING HELICOPTER BLADE

Ronaldo Vieira Cruz
Centro Técnico Aeroespacial (CTA/IAE)
ron.cruz@bol.com.br

Donizeti de Andrade
Instituto Tecnológico de Aeronáutica (ITA/IEAP)
donizeti@aer.ita.br

*Abstract. **This article analyses the stability in flutter of hovering helicopter blade. The equations of motion, coupled due to the offset of the blade section center of gravity when measured from the feathering axis, are obtained for the elastic blade case of the helicopter in hover and with an equivalent offset flap hinge. Numerical results from these equations involving design data, present within certification reports recently approved by the Fostering and Coordination Institute with the Brazilian Aerospace Technical Center, are shown as frequency and damping ratio diagrams, obtained as functions of the equivalent center of mass, to validate the present methodology with the manufacturer's corresponding outputs.***

Keywords. Hover, Helicopter Blade, Flutter, Stability.

Nomenclature

a	Two-dimensional lift curve slope, 1/rad
c	Blade chord, m
$c_{()}$	Cosine ( )
C'(k)	Theodorsen's lift deficiency function
D	Damping ratio
e	Flap hinge offset, m
$\overline{F}_z$	Aerodynamic force, $F_z/\rho_\infty\Omega^2(R-e)^2$, m
I_θ	Section moment of inertia about the feathering axis, $I_0+mx_l^2$, kg.m^2
K_{qj}	Geometry pitch-flap coupling
$\overline{L}$	Section aerodynamic lift force, $L/\rho_\infty\Omega^2(R-e)^2$, m
m	Blade mass per unit length, kg/m
$M_{()}, M_{(\cdot)}, M_{(\cdot\cdot)}$	Blade aerodynamic flap moment coefficient for hovering
$m_{()}, m_{(\cdot)}, m_{(\cdot\cdot)}$	Blade aerodynamic pitch moment about feathering axis coefficient for hovering
$m_{()e}, m_{(\cdot)e}, m_{(\cdot\cdot)e}$	Blade aerodynamic elastic torsion moment coefficient for hovering
$\overline{M}_a$	Section aerodynamic pitch moment, $M_a/\rho_\infty\Omega^2(R-e)^3$, m
M_F	Aerodynamic out-of-plane bending moment
M_f	Aerodynamic pitch moment
M_{fe}	Aerodynamic elastic torsion moment
$p_0(t)$	Rigid pitch degree of freedom
$p_k(t)$	Elastic torsion degrees of freedom
$q_k(t)$	Bending flap degrees of freedom
r	Blade radial coordinate, m
R	Blade radius, m
x, ρ	Section blade distance from the equivalent flap hinge offset, m
x_l	Chordwise offset of blade center of gravity behind pitch axis, m
$\eta_k(r)$	Bending flap mode shapes
υ_{kad}	Uncoupled natural frequency of *k*th out-of-plane bending mode, dimensionless
ω_{ad}	Uncoupled natural frequency of rigid pitch motion, $\omega_{ad}=K_\theta/I_f\Omega^2$, rad/s
Ω	Rotor rotational speed, rad/s
$\xi_k(r)$	Elastic torsion mode shapes
ρ_∞	Air density, kg/m^3
θ_0	Blade pitch angle at the blade root, rad
γ	Lock number, $\rho_\infty ac(R-e)^4/I_b$
$()^a$	Inertial quantity made dimensionless by I_b
$()^*$	$\partial/\partial\psi$ in dimensionless equations
$(^-)$	Length quantity made dimensionless by (R-e)

1. Introduction

In general, the term flutter refers to a dynamic instability, frequently a hazardous phenomenon, due to the structure-flow interaction. Historically, this term has been used to refer to an aeroelastic instability involving the coupled bending and torsion motion of a wing. For the rotary wing, flutter corresponds to the pitch-flap motion of the blade.

The rotation of the wing introduces a number of effects that make helicopter blade flutter much different from its fixed-wing counterpart. The centrifugal forces couple the flap and pitch motions if the center of gravity is offset from the feathering axis. Moreover, the returning shed wake has an important influence on the blade aerodynamic forces, as does the periodic aerodynamic environment of the blade in forward flight. This article, however, focuses at the hovering flight and considers quasi-steady aerodynamics. The influence of the returning shed wake is just contained within the induced angle of attack.

The classical problem considers two degrees of freedom, the rigid flap and rigid pitch motion of an articulated rotor blade. Since the control system is usually the most flexible element in the torsion motion, the rigid pitch degree of freedom is a good representation of the blade dynamics.

This article presents the coupled equations of motion for out-of-plane bending and elastic torsion of an articulated rotor blade in hover and with an equivalent offset flap hinge. It summarizes what is detailed on Cruz (2002). The structural operator is based on Johnson (1980), the aerodynamic operator on Hodges (1976), and the mode shapes for out-of-plane bending and elastic torsion are proposed by Karunamoorthy (1993) for an articulated rotor blade. The blade pitch mode is considered due to the control system flexibility. In these conditions, frequency and damping ratio diagrams, as functions of the equivalent center of mass, are obtained using design data, present within certification reports recently approved by the Fostering and Coordination Institute with the Brazilian Aerospace Technical Center.

After the design and the production of the blades, the manufacturer determines the mentioned diagrams in order to show the compliance with flutter requirements, which build up part of the helicopters certification process.

The international homologation authorities follow the certification requirements of their own countries. In Brazil, the small rotorcraft requirements up to 2730 kg are in RBHA 27 ("Requisitos Brasileiros de Homologação Aeronáutica"), while RBHA 29 establishes the requirements for large rotorcraft with maximum take off weight larger than 2730 kg. Both requirements establish the compliance of the corresponding American requirements, FAR (Federal Administration Regulation) 27 and 29 (2001).

With respect to flutter, the paragraph 629 of the FAR 27 and 29 establishes: "Each aerodynamic surface of the rotorcraft must be free from flutter under each appropriate speed and power condition". The paragraph 659, for its time, establishes: "The rotors and blades must be mass balanced as necessary to prevent excessive vibration and prevent flutter at any speed up to the maximum forward speed".

Consequently, the flutter analysis in the whole operational envelope of the rotorcraft is vital for the blade design. The manufacturer, before the first flight, has to foresee the possibility of this undesirable phenomenon because it can compromise the viability of the project and the safety of the prototype flight test crew.

So, it can be said that the steps for showing compliance with international aviation requirements are:

a) obtaining the frequency and damping ratio diagrams;

b) accomplishment of whirl blade tests for the practical determination of these frequencies and validation of the simulation results;

c) verification of the necessary actions involving the blade operation in order to prevent resonance in the normal regime of rotation; and

d) accomplishment of flight tests in order to check the vibration level in the whole flight envelope.

2. Coupled Equations of Motion

The procedure and the nomenclature presented by Johnson (1980) are used in order to obtain the coupled equations of motion for out-of-plane bending and elastic torsion of an articulated rotor blade in hover. Figure (1) presents the schematic drawing of the analyzed blade with an equivalent offset flap hinge. The chordwise position of the blade section of gravity is a distance x_l behind the feathering axis.
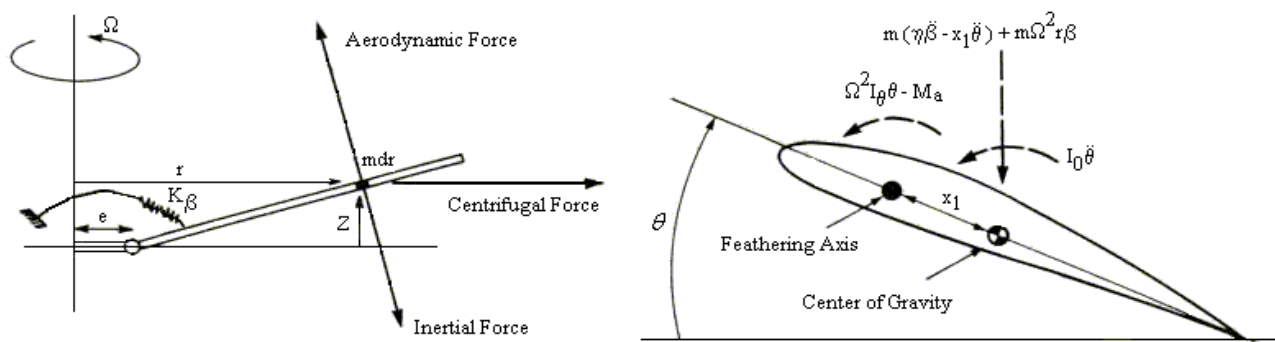

Figure 1. Blade model [Cruz (2002)].

It should be noticed that is not entirely consistent to exclude the in-plane motion from the torsion and out-of-plane bending motion of an elastic blade analysis. For example, the in-plane forces on the blade produce torsional moments when there is out-of-plane bending. In spite of it, the in-plane motion is not considered in this model.

It is assumed that the blade has a straight elastic axis coincident with the feathering axis and the built-in twist of the blade is not considered here, since it is only involved in the trim forces on the blade. The equations of motion are obtained from the conditions for equilibrium of moments on the blade outboard of r about the flap hinge, about the feathering axis and about the elastic axis. They are given by:

$$I_{qk}^a (q_k^{**} + \upsilon_{kad}^2 q_k) - \sum_{j=0}^{\infty} (I_{qk\ddot{p}j}^a p_j^{**} + I_{qkpj}^a p_j) = \gamma \int_0^1 \eta_k \frac{\overline{F}_z}{ac} d\overline{x} \; ; \tag{1}$$

$$I_{p0}^a (p_0^{**} + (\omega_{0ad}^2 + 1)p_0) + \sum_{j=1}^{\infty} I_{p0pj}^a (p_j^{**} + p_j) - \sum_{j=1}^{\infty} (I_{qj\ddot{p}0}^a q_j^{**} + I_{qjp0}^a q_j) = \gamma \int_0^1 \frac{\overline{M}_a}{ac} d\overline{x} - \sum_{j=1}^{\infty} I_{p0}^a \omega_{0ad}^2 K_{pj} q_j \; ; \text{ and} \tag{2}$$

$$I_{pk}^a (p_k^{**} + (\omega_{kad}^2 + 1)p_k) + I_{p0pk}^a (p_0^{**} + p_0) - \sum_{j=1}^{\infty} (I_{qj\ddot{p}k}^a q_j^{**} + I_{qjpk}^a q_j) = \gamma \int_0^1 \xi_k \frac{\overline{M}_a}{ac} d\overline{x} \; . \tag{3}$$

The inertial coefficients using dimensionless quantities (dividing by $I_b = \int_0^R mr^2 dr$) are:

$$I_{qk}^a = \frac{1}{I_b} \int_e^R \eta_k^2 m \, dr \; ; \tag{4}$$

$$I_{qk\ddot{p}j}^a = \frac{1}{I_b} \int_e^R \eta_k \xi_j x_1 m \, dr \; ; \tag{5}$$

$$I_{qkpj}^a = \frac{1}{I_b} \int_e^R x_1 m \int_e^r \eta_k' (\rho \xi_j)' d\rho \, dr \; ; \tag{6}$$

$$I_{pk}^a = \frac{1}{I_b} \int_e^R \xi_k^2 I_\theta \, dr \; ; \text{ and} \tag{7}$$

$$I_{popk}^a = \frac{1}{I_b} \int_e^R \xi_k I_\theta \, dr \; . \tag{8}$$

The bending and torsion equations are coupled by inertial and centrifugal forces if the section center of gravity is offset from the elastic axis. In order to solve these equations, it is necessary to develop their right hand side. That means to determine the aerodynamic terms as functions of the generalized coordinates of the problem.

Using the quasi-steady aerodynamic model proposed by Hodges (1976) and disconsidering the in-plane motion, the terms associates to precone, droop, sweep and torque offset, the non-linear terms, the influence of the profile drag at the generalized aerodynamic moment due rigid pitch deflection, the inflow terms, and the built-in twist of the blade, the aerodynamic out-of-plane bending, pitch and elastic torsion moments are respectively:

$$M_F = \int_0^1 \overline{\eta}_k \frac{\overline{F}_z}{ac} d\overline{x} = \sum_{j=0}^1 M_{pjqk} p_j + \sum_{j=0}^1 M_{\dot{p}jqk} p_j^* + \sum_{j=0}^1 M_{\ddot{p}jqk} p_j^{**} + \sum_{k=1}^3 M_{qk} q_k + \sum_{k=1}^3 M_{\dot{q}k} q_k^* + \sum_{k=1}^3 M_{\ddot{q}k} q_k^{**} \; ; \tag{9}$$

$$M_f = \int_0^1 \frac{\overline{M}_a}{ac} d\overline{x} = \sum_{j=0}^1 m_{pj} p_j + \sum_{j=0}^1 m_{\dot{p}j} p_j^* + \sum_{j=0}^1 m_{\ddot{p}j} p_j^{**} + \sum_{k=1}^3 m_{qk} q_k + \sum_{k=1}^3 m_{\dot{q}k} q_k^* + \sum_{k=1}^3 m_{\ddot{q}k} q_k^{**} \; ; \text{ and} \tag{10}$$

$$M_{fe} = \int_0^1 \xi_k \frac{\overline{M}_a}{ac} d\overline{x} = \sum_{j=0}^1 m_{pje} p_j + \sum_{j=0}^1 m_{\dot{p}je} p_j^* + \sum_{j=0}^1 m_{\ddot{p}ke} p_j^{**} + \sum_{k=1}^3 m_{qke} q_k + \sum_{k=1}^3 m_{\dot{q}ke} q_k^* + \sum_{k=1}^3 m_{\ddot{q}ke} q_k^{**} \; . \tag{11}$$

For hover, the aerodynamic coefficients are:

$$M_{poqk} = \frac{1}{2}\int_0^1 \overline{\eta}_k(\overline{x}^2 + 2\overline{ex})c_{2\theta_0}d\overline{x} \; ; \tag{12}$$

$$M_{\dot{p}0qk} = \frac{3}{8}\int_0^1 \overline{\eta}_k\,\overline{cx}c_{\theta_0}d\overline{x} \; ; \tag{13}$$

$$M_{p1qk} = \frac{1}{2}\int_0^1 \overline{\eta}_k(\overline{x}^2 + 2\overline{ex})\xi_1(\overline{x})c_{\theta_0}^2 d\overline{x} \; ; \tag{14}$$

$$M_{\dot{p}1qk} = \frac{3}{8}\int_0^1 \overline{\eta}_k\,\overline{cx}\xi_1(\overline{x})c_{\theta_0}d\overline{x} \; ; \tag{15}$$

$$M_{qk} = \frac{1}{4}\int_0^1 \overline{\eta}_k\,\overline{cx}\eta_k'(\overline{x})c_{\theta_0}^2 d\overline{x} \; ; \tag{16}$$

$$M_{\dot{q}k} = -\frac{1}{2}\int_0^1 (\overline{x}+\overline{e})\overline{\eta}_k^2(\overline{x})c_{\theta_0}d\overline{x} \; ; \tag{17}$$

$$M_{\ddot{q}k} = -\frac{1}{8}\int_0^1 \overline{\eta}_k^2(\overline{x})\overline{c}d\overline{x} \; ; \tag{18}$$

$$m_{\dot{p}0} = -\frac{1}{16}\int_0^1 \overline{c}^2\,\overline{x}c_{\theta_0}d\overline{x} \; ; \tag{19}$$

$$m_{\dot{p}1} = -\frac{1}{16}\int_0^1 \overline{c}^2\,\overline{x}\xi_1(\overline{x})c_{\theta_0}d\overline{x} \; ; \tag{20}$$

$$m_{qk} = -\frac{1}{32}\int_0^1 \overline{c}^2\,\overline{x}\eta_k'(\overline{x})c_{\theta_0}^2 d\overline{x} \; ; \tag{21}$$

$$m_{\ddot{q}k} = \frac{1}{32}\int_0^1 \overline{c}^2\,\overline{\eta}_k(\overline{x})d\overline{x} \; ; \tag{22}$$

$$m_{\dot{p}0e} = -\frac{1}{16}\int_0^1 \overline{c}^2\,\overline{x}\xi_1(\overline{x})c_{\theta_0}d\overline{x} \; ; \tag{23}$$

$$m_{\dot{p}1e} = -\frac{1}{16}\int_0^1 \overline{c}^2\,\overline{x}\xi_1^2(\overline{x})c_{\theta_0}d\overline{x} \; ; \tag{24}$$

$$m_{qke} = -\frac{1}{32}\int_0^1 \overline{c}^2\,\overline{x}\eta_k'(\overline{x})\xi_1(\overline{x})c_{\theta_0}^2 d\overline{x} \; ; \; e \tag{25}$$

$$m_{\ddot{q}ke} = \frac{1}{32}\int_0^1 \overline{c}^2\,\overline{\eta}_k(\overline{x})\xi_1(\overline{x})d\overline{x} \; . \tag{26}$$

The $M_{\dot{p}0qk}$, $M_{\dot{p}1qk}$, m_{p0}, $m_{\dot{p}0}$, m_{p1}, $m_{\dot{p}1}$, $m_{\dot{q}k}$, m_{p0e}, $m_{\dot{p}0e}$, m_{p1e}, $m_{\dot{p}1e}$ e $m_{\dot{q}ke}$ terms vanish and the mode shapes of out-of-plane bending and elastic torsion are the polynomials proposed by Karunamoorthy (1993) for an articulated rotor blade - Tab. (1) and (2).

Table 1: Coefficients for pinned-free flexural polynomials: $\eta_n = (C_1 x + C_2 x^3 + C_3 x^4 + \ldots)/\Delta n$.

n	$\overline{x}$	$\overline{x}^3$	$\overline{x}^4$	$\overline{x}^5$	$\overline{x}^6$	1
1	1					1
2	-16	70	-70	21		5
3	648	-10910	24510	-19593	5440	95

Table 2: Coefficients for free-free torsional polynomials: $\xi_{n-1} = (C_1 + C_2 x^2 + C_3 x^3 + \ldots)/\Delta n$.

n	$\bar{x}^0$	$\bar{x}^2$	$\bar{x}^3$	$\bar{x}^4$	Δn
1	1				1
2	-1	6	-4		1
3	1	-30	60	-30	1

3. Frequency and Modal Damping Diagrams

The coupled equations of motion for out-of-plane bending and elastic torsion of an articulated rotor blade in hover consist of a second order homogeneous linear differential equations system with constant coefficients. They are given by

$$[M]\{y\}^{**} + [C]\{y\}^{*} + [K]\{y\} = \{0\}, \tag{27}$$

where

$$[M] = \begin{bmatrix} I^a_{q1} - \gamma M_{\ddot{q}1} & -\gamma M_{\ddot{q}2} & -\gamma M_{\ddot{q}3} & -I^a_{q1\ddot{p}0} - \gamma M_{\ddot{p}0q1} & -I^a_{q1\ddot{p}1} - \gamma M_{\ddot{p}1q1} \\ -\gamma M_{\ddot{q}1} & I^a_{q2} - \gamma M_{\ddot{q}2} & -\gamma M_{\ddot{q}3} & -I^a_{q2\ddot{p}0} - \gamma M_{\ddot{p}0q2} & -I^a_{q2\ddot{p}1} - \gamma M_{\ddot{p}1q2} \\ -\gamma M_{\ddot{q}1} & -\gamma M_{\ddot{q}2} & I^a_{q3} - \gamma M_{\ddot{q}3} & -I^a_{q3\ddot{p}0} - \gamma M_{\ddot{p}0q3} & -I^a_{q3\ddot{p}1} - \gamma M_{\ddot{p}1q3} \\ -I^a_{q1\ddot{p}0} - \gamma m_{\ddot{q}1} & -I^a_{q2\ddot{p}0} - \gamma m_{\ddot{q}2} & -I^a_{q3\ddot{p}0} - \gamma m_{\ddot{q}3} & I^a_{p0} - \gamma m_{\ddot{p}0} & I^a_{p0p1} - \gamma m_{\ddot{p}1} \\ -I^a_{q1\ddot{p}1} - \gamma m_{\ddot{q}1e} & -I^a_{q2\ddot{p}1} - \gamma m_{\ddot{q}2e} & -I^a_{q3\ddot{p}1} - \gamma m_{\ddot{q}3e} & I^a_{p0p1} - \gamma m_{\ddot{p}0e} & I^a_{p1} - \gamma m_{\ddot{p}1e} \end{bmatrix}, \tag{28}$$

$$[C] = \begin{bmatrix} -\gamma M_{\dot{q}1} & -\gamma M_{\dot{q}2} & -\gamma M_{\dot{q}3} & -\gamma M_{\dot{p}0q1} & -\gamma M_{\dot{p}1q1} \\ -\gamma M_{\dot{q}1} & -\gamma M_{\dot{q}2} & -\gamma M_{\dot{q}3} & -\gamma M_{\dot{p}0q2} & -\gamma M_{\dot{p}1q2} \\ -\gamma M_{\dot{q}1} & -\gamma M_{\dot{q}2} & -\gamma M_{\dot{q}3} & -\gamma M_{\dot{p}0q3} & -\gamma M_{\dot{p}1q3} \\ -\gamma m_{\dot{q}1} & -\gamma m_{\dot{q}2} & -\gamma m_{\dot{q}3} & -\gamma m_{\dot{p}0} & -\gamma m_{\dot{p}1} \\ -\gamma m_{\dot{q}1e} & -\gamma m_{\dot{q}2e} & -\gamma m_{\dot{q}3e} & -\gamma m_{\dot{p}0e} & -\gamma m_{\dot{p}1e} \end{bmatrix}, \tag{29}$$

$$[K] = \begin{bmatrix} I^a_{q1}\upsilon^2_{1ad} - \gamma M_{q1} & -\gamma M_{q2} & -\gamma M_{q3} & -I^a_{q1p0} - \gamma M_{p0q1} & -I^a_{q1p1} - \gamma M_{p1q1} \\ -\gamma M_{q1} & I^a_{q2}\upsilon^2_{2ad} - \gamma M_{q2} & -\gamma M_{q3} & -I^a_{q2p0} - \gamma M_{p0q2} & -I^a_{q2p1} - \gamma M_{p1q2} \\ -\gamma M_{q1} & -\gamma M_{q2} & I^a_{q3}\upsilon^2_3 - \gamma M_{q3} & -I^a_{q3p0} - \gamma M_{p0q3} & -I^a_{q3p1} - \gamma M_{p1q3} \\ -I^a_{q1p0} + I^a_{p0}\omega^2_{0ad}K_p - \gamma m_{q1} & -I^a_{q2p0} + I^a_{p0}\omega^2_{0ad}K_p - \gamma m_{q2} & -I^a_{q3p0} + I^a_{p0}\omega^2_{0ad}K_p - \gamma m_{q3} & I^a_{p0}(\omega^2_{0ad}+1) - \gamma m_{p0} & I^a_{p0p1} - \gamma m_{p1} \\ -I^a_{q1p1} - \gamma m_{q1e} & -I^a_{q2p1} - \gamma m_{q2e} & -I^a_{q3p1} - \gamma m_{q3e} & I^a_{p0p1} - \gamma m_{p0e} & I^a_{p1}(\omega^2_{1ad}+1) - \gamma m_{p1e} \end{bmatrix}, \text{ and} \tag{30}$$

$$\{y\} = \begin{Bmatrix} q_1 \\ q_2 \\ q_3 \\ p_0 \\ p_1 \end{Bmatrix}. \tag{31}$$

The state variable representation for this system of equations can be written as

$$[J]\{x\}^{*} + [A]\{x\} = \{0\} \quad \Rightarrow \quad \{x\}^{*} = [J]^{-1}[A]\{x\} \equiv [L]\{x\}, \tag{32}$$

where

$$[J] = \begin{bmatrix} 0 & [M] \\ [I] & 0 \end{bmatrix}, \quad [A] = \begin{bmatrix} [K] & [C] \\ 0 & [-I] \end{bmatrix}, \quad \{x\} = \begin{Bmatrix} \{y\}^{*} \\ \{y\} \end{Bmatrix} \text{ and} \tag{33}$$

[L] is a constant coefficient matrix for each x_l.

The stability of the dynamic system depends upon the solution of constant coefficient differential equations, yielding a solution of the type

$$\{x\} = \{\varphi_i\}e^{\lambda_i \bar{t}},\tag{34}$$

where one observes that λ_i and $\{\varphi_i\}$ are the eigenvalues and eigenvectors of the stability matrix [L], respectively. In general, λ_i is complex, and can be written as

$$\lambda_i = \delta \pm i\omega,\tag{35}$$

where δ is the modal damping and ω is the modal frequency.

Therefore, the damping ratio (D) can be represented for

$$D = -\delta / \sqrt{\delta^2 + \omega^2}.\tag{36}$$

Using these expressions, the frequency and modal damping diagrams of the blades can be obtained as a function of the chordwise distance of the blade section of gravity behind the feathering axis (x_l).

4. Results and Discussion

Using MATLAB (1995), numerical results from the flutter analysis of the elastic blade are obtained in hover. These results are divided in two cases: out-of-plane bending and pitch motions (no-elastic torsion case) and out-of-plane bending, pitch and elastic torsion motions (elastic torsion case).

In both cases the frequency and modal damping diagrams are presented as functions of the equivalent center of mass. These diagrams are obtained using design data, present within certification reports recently approved by the Fostering and Coordination Institute with the Brazilian Aerospace Technical Center. The manufacturer's results are shown in order to compare and validate the present methodology. The influence of the blade pitch angle at the blade root defined by pilot command as a function of the weight and altitude-density and the influence of the rotor rotational speed are also considered.

4.1. No-Elastic Torsion Case

Figures (2) and (3) present the frequency and modal damping diagrams as a function of the equivalent center of mass position in hover. The blade is assumed to have zero pitch angle and 100% of the rotor rotational speed.

Figure (2a) shows that the frequencies of the three flap modes and the frequency of the pitch mode are quite far from each other, while Fig. (3a) shows that all modal damping diagrams are positive. It means that the system is stable in all positions of the equivalent center of mass from 25 to 35% and, consequently, in the rotorcraft design condition, represented by the vertical line, at the 26.8% of the equivalent center of mass position.
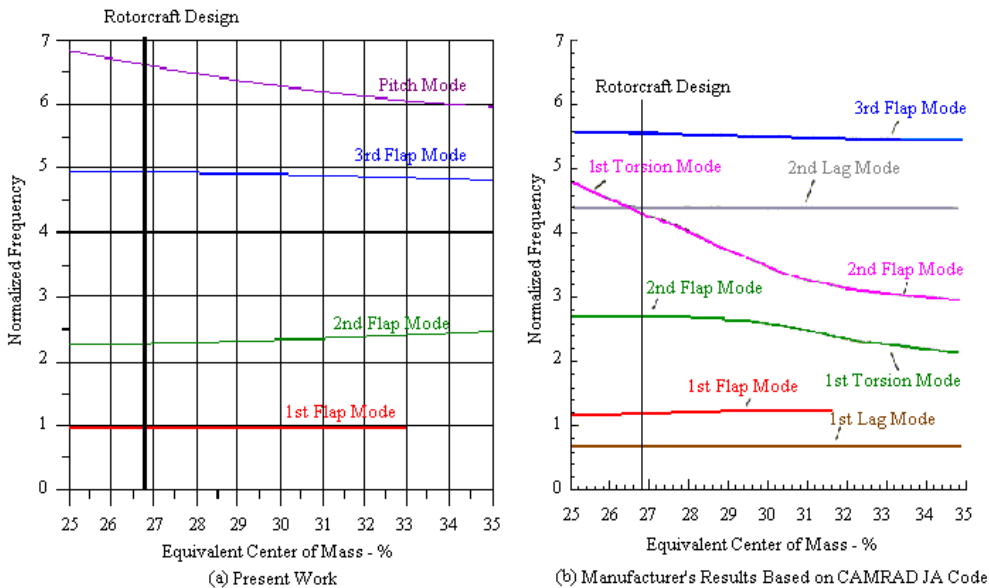

Figure 2. Frequency diagram for the no-elastic torsion case at zero pitch angle and 100% of the rotor rotational speed.
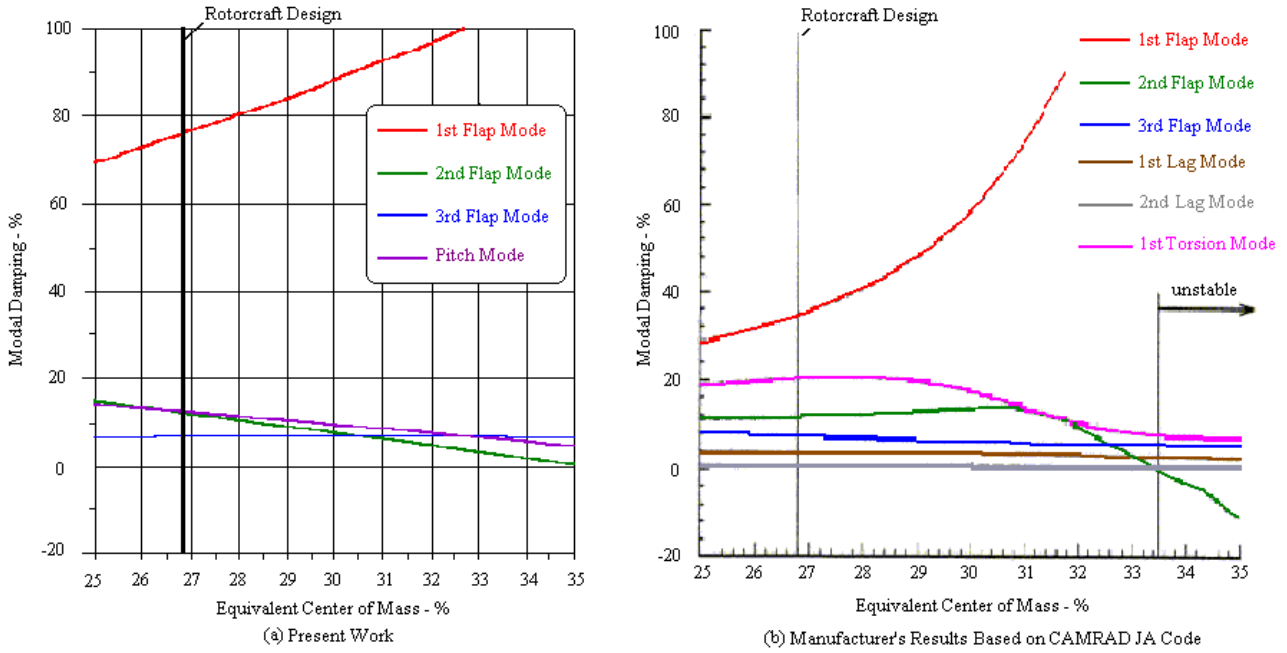
Figure 3. Modal damping diagram for the no-elastic torsion case at zero pitch angle and 100% of the rotor speed.

In order to validate the methodology, numerical results obtained by the computational simulation are compared with the manufacturer's corresponding outputs shown in Fig. (2b) and (3b). The frequencies and modal damping diagrams of the first and the third flap mode are quite similar in both simulations. The third flap mode is practically constant, while the first mode tends to reach 100% modal damping at approximately 32% of the equivalent center of mass position, according to Fig. (3).

Figure (2a) doesn't show the frequency coalescence between the second flap mode and the first torsion mode, because this simulation corresponds to the no-elastic torsion case. However, for the control system of the studied aircraft is very rigid, the pitch mode frequency is very high and, therefore, it doesn't affect the system stability. This conclusion is in agreement with the results presented by the manufacturer.

For these reasons, considering a simplified rotor model with no-elastic torsion, the methodology presented in this article is valid, but it shall be recognized that a further analysis involving torsional elastic effects must be pursued.

The influence of the blade pitch angle at the blade root defined by pilot command and the influence of the rotor rotational speed are also considered. Table (3) presents the modal damping values of each simulated configuration in the rotorcraft design condition at the 26.8% of the equivalent center of mass position.

Table 3: Modal damping values at the design condition (no-elastic torsion case).

Condition	Modal Damping (%)			
	1º Flap Mode	2º Flap Mode	3º Flap Mode	Pitch Mode
$\theta_0 = 0$ and $\Omega = 100\%$	75.6	12.2	6.77	12.5
$\theta_0 = 15º$ and $\Omega = 100\%$	72.5	12.6	6.58	12.1
$\theta_0 = 0$ and $\Omega = 104\%$	72.1	11.9	6.78	12.7

Table (3) allows the numerical analysis of the system stability as functions of the pitch cyclic position and of the rotor rotational speed. In the rotorcraft design condition, even with extreme values of blade pitch angle and rotation regime, a great safety margin exists. It means that the probability of occurrence of the flutter in hover is highly remote. Fig. (2) and (3) show that the second flap mode is the most critical. So, Table (3) also allows a quick analysis of the most critical flight condition regarding flutter, which corresponds to 104% of the rotation regime and zero blade pitch angle condition because it corresponds the smallest value of modal damping at the most critical mode.

4.2. Elastic Torsion Case

Figures (4) and (5) present the frequency and modal damping diagrams as a function of the equivalent center of mass position for the elastic torsion case in hover. The blade is assumed to have zero pitch angle and 100% of rotor rotational speed.
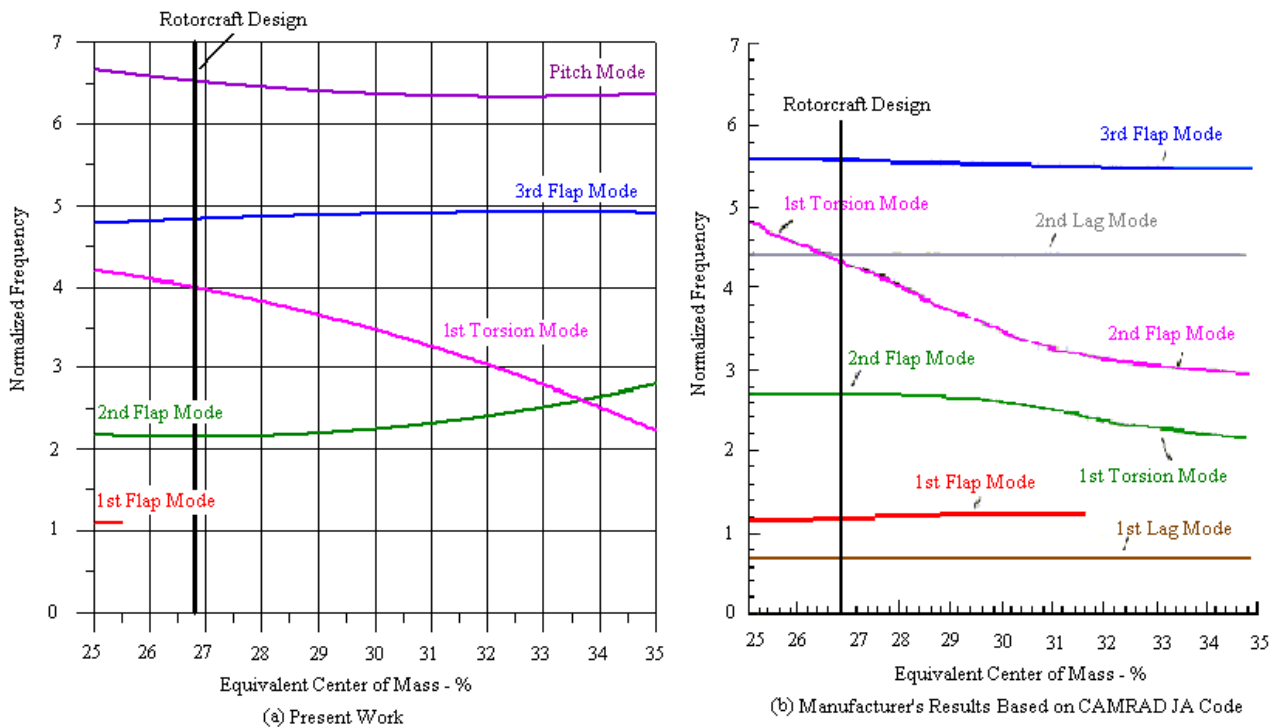
Figure 4. Frequency diagram for the elastic torsion case at zero pitch angle and 100% of the rotor rotational speed.
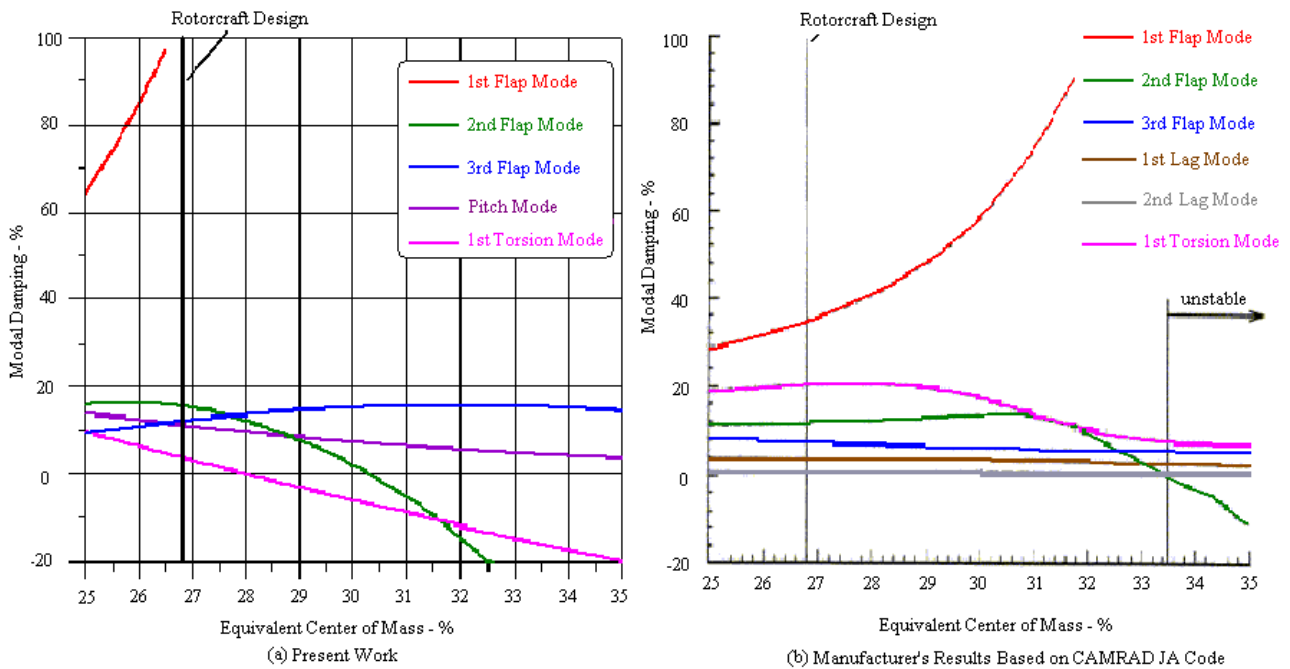

Figure 5. Modal damping diagram for the elastic torsion case at zero pitch angle and 100% of the rotor rotational speed.

Figure (4a) shows that the second flap mode frequency coalesces with the frequency of the first torsion mode approximately at the 33.5% of the equivalent center of mass position. This result is in agreement with the manufacturer's corresponding outputs as shown in Fig. (4b) and (5b). However, the other results of the present methodology, shown in Fig. (5a), are quite different from the manufacturer's outputs presented in Fig. (5b). The system becomes unstable at the 28% of the equivalent center-of-mass position instead of 33.5%.

Another discrepancy refers to the first flap mode. Figure (5b) shows that the modal damping tends to reach 100% at the 32% of the equivalent center of mass position. For the present methodology, the modal damping reaches this value early, at the approximately 27% of the equivalent center of mass position, as shown in Fig. (5a).

These discrepancies from the numerical results and the manufacturer's corresponding outputs are attributed to the following factors:

a) use of an articulated rotor blade model with an equivalent offset flap hinge instead of the bearingless model used by the manufacturer;

b) disregard of the in-plane motion on the structural model;

c) disregard of the non-linear terms and of the influence of the profile drag at the generalized aerodynamic moment due to rigid pitch deflection;

d) use of a quasi-steady aerodynamic model, where the influence of the returning shed wake is just contained within the induced angle of attack (unsteady effects are not considered); and

e) design data present within certification reports are often simplified and can be inaccurate.

Even though damping results are different from the manufacturer's, the frequency diagram for the elastic case presented on Fig.(4a) show mode coalescence around the same equivalent center of mass position as the manufacturer's. Since this is the determining phenomenon in this case with respect to when the system will become unstable, the present work's results actually give a consistent indication of where the instability boundary would be, at least in terms of the frequency results.

It should be noticed that the manufacturer's final conclusion for the results presented on Fig. (5b) can also be obtained by the analysis of Fig. (4a) and (5a). It can be observed that the third flap mode, the pitch mode frequency and the elastic mode frequencies are quite far from each other and the modal damping ratios are positive, characterizing a stable system, on the rotorcraft design condition represented by the vertical line (26.8% of the equivalent center of mass position).

The influence of the blade pitch angle at the blade root defined by pilot command and the influence of the rotor rotational speed are also considered for elastic torsion case. Table (4) presents the modal damping values of each simulated configuration in the rotorcraft design condition at the 26.8% of the equivalent center of mass position.

Table 4: Modal damping values at the design condition (elastic torsion case).

Condition	Modal Damping (%)				
	1º Flap Mode	2º Flap Mode	3º Flap Mode	Pitch Mode	1º Torsion Mode
$\theta_0 = 0$ and $\Omega = 100\%$	100	13.0	13.1	11.2	5.08
$\theta_0 = 15°$ and $\Omega = 100\%$	98.3	14.0	12.2	11.0	5.94
$\theta_0 = 0$ and $\Omega = 104\%$	98.8	13.7	12.1	11.1	5.75

Table (4) allows the numerical analysis of the system stability as functions of the pitch cyclic position and of the rotor rotational speed. In the rotorcraft design condition, even with extreme values of blade pitch angle and rotation regime, a great safety margin exists. It means that the probability of occurrence of the flutter in hover is highly remote. Considering that the most critical mode is the second flap mode, as observed for the previous case, Tab. (4) also allows a quick analysis of the most critical flight condition regarding flutter, which corresponds to 100% of the rotation regime and zero blade pitch angle condition, because it corresponds to the smallest value of modal damping at the most critical mode.

The determination of the most conservative flight condition is useful because it permits to plan a gradual approach to this condition on the prototype flight tests, increasing safety. This condition is presented within certification reports of each rotorcraft.

Finally, it shall be noticed that the manufacturer must show compliance with the flutter requirements in the whole flight envelope for international aviation authorities in order to certificate the rotorcraft. This article focuses at the hovering flight; however, the manufacturer has to simulate and, mainly, fly the aircraft in each flight condition.

5. Conclusions

The numerical results from the coupled equations of motion for out-of-plane bending and elastic torsion of an articulated rotor blade in hover, considering a quasi-steady aerodynamic model, are obtained by MATLAB (1995).

For out-of-plane bending and pitch motions (no-elastic torsion case), the numerical results of the frequency and modal damping diagrams are quite similar to the manufacturer's corresponding outputs present within certification reports, regarding to the bending flap modes.

For out-of-plane bending, pitch and elastic torsion motions (elastic torsion case), the numerical results of the frequency diagram are quite similar to the manufacturer's corresponding outputs present within certification reports; however, the numerical results of the modal damping diagram are quite different. These discrepancies from the numerical results are attributed to the structural and aerodynamic model simplifications and to the possible inaccuracy of the certification data reports. Even though damping results are different from the manufacturer's, the frequency diagram for the elastic case show mode coalescence around the same equivalent center of mass position as the manufacturer's. Since this is the determining phenomenon in this case with respect to when the system will become unstable, the present work's results actually give a consistent indication of where the instability boundary would be, at least in terms of the frequency results.

Both cases show that there is not occurrence of flutter for the whole range of rotation regime and the collective command position on the rotorcraft design condition (26.8% of the equivalent center of mass position). It is in agreement with the manufacturer's final conclusion present within certification reports. For the most general case, it is also verified that the most conservative analysis condition is the zero pitch and 100% rotor rotational speed condition.

6. References

Cruz, R.V., 2002, "Estabilidade em Flutter de Pás de Rotores de Helicópteros em Vôo Pairado – Um Estudo de Caso", Master Degree Thesis, Technological Institute of Aeronautics, São José dos Campos, Brazil.

Federal Aviation Administration, 2001, "FAR 27: Airworthiness Standards: Normal Category Rotorcraft", Washington, DC.

Federal Aviation Administration, 2001, "FAR 29: Airworthiness Standards: Transport Category Rotorcraft", Washington, DC.

Hodges, D. H., 1976, "Nonlinear Equations of Motion for Cantilever Rotor Blades in Hover with Pitch Link Flexibility, Twist, Precone, Droop, Sweep, Torque Offset, and Blade Root Offset", NASA TM X-73, 112, Washington, DC.

Johnson, W., 1980, "Helicopter Theory", Princeton Univ. Press, Princeton, NJ, pp. 378-709.

Karunamoorthy, S. N., 1993, "Orthogonal Polynomials in Rotary Wing Structural Dynamics", Journal of the American Helicopter Society, v.38, n.3, pp.93-98.

Matlab, 1995, "High-Performance Numeric Computation and Visualization Software: User's Guide", The MathWorks Inc., Natick, Massachusetts.

7. Copyright Notice